

A Search for Ultraviolet Emission from LINERs

Aaron J. Barth

Department of Astronomy, University of California, Berkeley CA 94720-3411

Luis C. Ho

Harvard-Smithsonian Center for Astrophysics, 60 Garden Street, Cambridge, MA 02138

Alexei V. Filippenko

Department of Astronomy, University of California, Berkeley CA 94720-3411

Wallace L. W. Sargent

Palomar Observatory, 105-24 Caltech, Pasadena, CA 91125

ABSTRACT

We have obtained *Hubble Space Telescope* Wide Field and Planetary Camera 2 ultraviolet (UV) 2200 Å and optical *V*-band images of 20 low-luminosity active galactic nuclei, most of which are spectroscopically classified as LINERs, in order to search for a possible photoionizing continuum. Six (30%) of the galaxies are detected in the UV. Two of the detected galaxies (NGC 3642 and NGC 4203) have compact, unresolved nuclear UV sources, while the remaining four UV sources (in NGC 4569, NGC 5005, NGC 6500, and NGC 7743) are spatially extended. Combining our sample with that of Maoz et al. (1995), we find that the probability of detection of a nuclear UV source is greatest for galaxies having low internal reddening and low inclination, and we conclude that dust obscuration is the dominant factor determining whether or not a UV source is detected. Large emission-line equivalent widths and the presence of broad-line emission also increase the likelihood of detection of nuclear UV emission. Our results suggest that the majority of LINERs harbor obscured nuclear UV sources, which may be either accretion-powered active nuclei or young star clusters. Under the assumption that the compact UV sources in NGC 3642 and NGC 4203 have nonstellar spectra of slope $f_\nu \propto \nu^{-1}$ extending into the extreme ultraviolet, the extrapolated ionizing fluxes are sufficiently strong to photoionize the narrow-line regions of these objects. The *V*-band images of many galaxies in our sample reveal remarkably strong dust lanes which may be responsible for obscuring some UV sources.

Subject headings: galaxies: active — galaxies: nuclei — ultraviolet: galaxies

To appear in *The Astrophysical Journal*.

1. Introduction

Emission-line galactic nuclei are generally classified into three major categories: star-forming or H II nuclei, in which young, massive stars provide the photoionizing continuum; Seyfert nuclei, which are generally understood to be the result of accretion onto a supermassive black hole; and low-ionization nuclear emission-line regions, or LINERs, which were first defined as a class by Heckman (1980). Despite much observational and theoretical study, understanding the excitation mechanism of LINERs has proved to be an elusive goal. Optical spectroscopy alone does not provide sufficient constraints to determine unambiguously the nature of LINERs. Models based on shock excitation (Koski & Osterbrock 1976; Fosbury et al. 1978; Dopita & Sutherland 1995, 1996), photoionization by hot stars (Terlevich & Melnick 1985; Filippenko & Terlevich 1992; Shields 1992), and photoionization by a nonstellar power-law continuum (Ferland & Netzer 1983; Halpern & Steiner 1983; Ho, Filippenko, & Sargent 1993) have all had reasonable success at reproducing the optical emission-line ratios of LINERs. There are compelling reasons to believe that all of these mechanisms may play a role, but it is not known which mechanism dominates in the majority of LINERs.

At the heart of the subject is the fundamental question of whether LINERs are powered by accretion onto a black hole, or by massive stars, or by some other process. Ultraviolet (UV) observations can shed light on this issue in several ways. If a cluster of young stars is present, then it should be possible to detect UV spectroscopic signatures of massive stars such as P Cygni line profiles. On the other hand, an accretion-powered object, if not obscured by dust, should manifest itself as a spatially unresolved source of a featureless UV continuum, possibly accompanied by the broad emission lines that are the signature of Seyfert and quasar activity.

A UV imaging survey using the pre-refurbishment *Hubble Space Telescope (HST)* Faint Object Camera (FOC) and F220W filter (Maoz et al. 1995) has shown that about 20% of nearby LINERs harbor a source of UV emission with a diameter of at most several parsecs. Without spectroscopy, compact young star clusters cannot be ruled out as the sources of the emission, but this result is highly suggestive of the existence of genuine AGN-like featureless continua in at least some LINERs. Assuming an $f_\nu \propto \nu^{-1}$ continuum, Maoz et al. find that the inferred ionizing luminosity is sufficient to power the observed emission lines. Maoz et al. proposed three possible explanations for the low UV detection rate. The majority of LINERs in which UV emission is not detected could be shock excited rather than photoionized; they could contain UV sources which are obscured by dust; or, the central photoionizing source could be “turned off” the majority of the time. Eracleous, Livio, & Binette (1995) have explored this third possibility by proposing a model in which the occasional disruption of a star by the central massive black hole leads to the formation of an accretion disk lasting a few decades, providing the energy source for the LINER, while the emission lines decay on 100-year timescales. Of course, these possible explanations are not mutually exclusive, and they all may play a role in determining the observed UV properties of LINERs.

In order to further constrain the excitation mechanism of LINERs, and to discover more

candidates for UV spectroscopy, we have carried out an *HST* UV and optical imaging survey using the Wide Field and Planetary Camera 2 (WFPC2). In agreement with the results of the Maoz et al. survey, we find that the majority of the nuclei in our sample are completely dark in the UV. Among the objects showing UV emission, we find that two have unresolved nuclear sources which are sufficiently bright to account for the emission-line fluxes by photoionization. The remaining four UV-detected nuclei are spatially extended sources. By combining our dataset with that of Maoz et al., we are able to assemble a sample of galaxies large enough to study the relationships between the UV detection rate and overall host galaxy properties such as inclination, reddening, and emission-line ratios.

2. Sample Selection and Observations

The galaxy sample consists of 20 LINERs, low-luminosity Seyfert 2 nuclei, and LINER/H II “transition” objects selected from the Palomar Observatory Dwarf Seyfert Survey (Filippenko & Sargent 1985; Ho, Filippenko, & Sargent 1995). Objects were selected on the basis of having weak or undetected broad H α emission; the detailed profile-fitting analysis carried out by Ho et al. (1997b) has subsequently detected broad H α emission in five of these galaxies. Based on the classifications of Ho, Filippenko, & Sargent (1997a), the sample contains 14 LINERs, 3 Seyfert 2s, and 3 LINER/H II transition objects. The galaxies span a range in Hubble types from S0 to Sc, and the median redshift of the sample is $cz = 1070 \text{ km s}^{-1}$. Five galaxies in this sample were also observed as part of the FOC UV snapshot survey of Maoz et al. (1995). Table 1 lists the basic galaxy parameters and the WFPC2 exposure times.

The galaxies were observed between May 1994 and March 1995, through the F218W filter (mean wavelength 2190 Å, effective width 390 Å), with the nucleus placed on the Planetary Camera CCD (pixel scale 0".046, field of view 35" \times 35"). Exposures were split into two separate integrations to facilitate cosmic-ray removal, and total exposure times ranged from 1400 to 2200 s. Brief (230–350 s) single exposures in the F547M (*V* band) filter were also obtained to verify pointing, to examine the optical morphology of the nuclei, and to constrain the red leak contribution to the UV signal. Bias subtraction and flat-fielding were performed by the standard *HST* data calibration pipeline. Figure 1 shows the F218W images of the UV-detected nuclei, and the F547M images are displayed in Figure 2.

For the UV images, cosmic ray removal and averaging of the two sub-exposures were performed using the CRREJECT task in IRAF¹. We removed cosmic-ray hits from the F547M images by replacing abnormally high pixels with the average count level found in neighboring pixels, using the IRAF COSMICRAYS task, but many residuals and faint streaks remain in the images.

¹IRAF is distributed by the National Optical Astronomy Observatories, which are operated by the Association of Universities for Research in Astronomy, Inc., under cooperative agreement with the National Science Foundation.

Distances to the galaxies, when needed, were obtained from the Nearby Galaxies Catalog (Tully 1988), which assumes a Hubble constant of $H_0 = 75 \text{ km s}^{-1} \text{ Mpc}^{-1}$ and the Virgo infall model of Tully & Shaya (1984). For NGC 6500, which is too distant to appear in the catalog, we computed the distance using $H_0 = 75 \text{ km s}^{-1} \text{ Mpc}^{-1}$.

3. Results

3.1. UV Detection Rate

After cosmic-ray cleaning, we blinked the UV and optical images of each galaxy against each other to determine by eye whether UV emission was detected at the nucleus. Most images proved to be completely blank in the UV; only four clearly showed nuclear UV emission, while two others showed extremely weak features at the nucleus. Off-nuclear clusters of hot stars or foreground Galactic stars were visible in a few others. Because the UV and optical images of each galaxy were obtained in a single telescope pointing, the position of the nucleus on the PC detector should be the same in the UV and optical exposures. We found this to be the case for each of the UV-detected galaxies.

We performed photometry on the F218W images of the UV-detected galaxies using DAOPHOT (Stetson 1987). Total F218W counts were measured in a circular aperture large enough to surround all the detected flux from each nuclear source. Count rates were then converted to continuum fluxes at 2200 \AA using the relation that 1 count s^{-1} is equivalent to $f_\lambda(2200 \text{ \AA}) = 1.03 \times 10^{-15} \text{ erg cm}^{-2} \text{ s}^{-1} \text{ \AA}^{-1}$. This conversion was determined by performing synthetic photometry on a power-law continuum with $f_\nu \propto \nu^{-1}$ using the F218W transmission curve in the IRAF SYNPHOT package. We found that varying the power-law slope by ± 1 or substituting an O-type stellar continuum resulted in variations of $< 5\%$ in the counts-to-flux conversion.

Count rates were also corrected for the time-dependent WFPC2 throughput, which varies due to the buildup of contaminants in the camera optics. The mean throughput correction was 5%, and no observation required a correction of greater than 10%. Extinction corrections were computed using the reddening estimates of Burstein & Heiles (1984) and the Galactic reddening curve of Cardelli, Clayton, & Mathis (1989). The measured and extinction-corrected fluxes are listed in Table 2.

Two of the UV-detected galaxies, NGC 3642 and NGC 4203, contain nuclear sources that appear pointlike, or nearly so, but there is clearly some faint extended UV emission surrounding the nucleus of NGC 3642. Figure 3 shows the photometric growth curves for these two sources and for an artificial point-spread function (PSF) created using TINY TIM (version 3.0a; Krist 1994), normalized to the same magnitude within a radius of $r = 1$ pixel. The profiles of NGC 3642 and 4203 are nearly identical out to $r = 2$ pixels radius, and are only marginally more extended than the artificial PSF. We conclude that the cores of these sources ($r \leq 2$ pixels) are not resolved by

HST. At larger radii ($r > 3$ pixels), the profiles reveal the presence of spatially extended emission, particularly in NGC 3642. By comparing the radial profiles of the UV sources with those of artificially broadened PSFs, we estimate that the cores of these sources, which dominate the light at $r \leq 2$ pixels radius, have intrinsic widths of < 0.5 pixel full-width at half-maximum (FWHM). The corresponding physical size limits are < 3.1 pc and < 1.1 pc FWHM at the distances of NGC 3642 and NGC 4203 (27.5 and 9.7 Mpc, respectively).

The other two easily detected galaxies, NGC 4569 and NGC 6500, are clearly extended sources. The UV-emitting region in NGC 6500 is a diffuse patch without a bright central core. In NGC 4569, the UV source is centrally peaked but elongated along PA $\approx 20^\circ$; the photometric growth curve illustrated in Figure 3 shows that it is more extended than the UV sources in NGC 3642 and NGC 4203. Its FWHM size is 13×9 pc² along its major and minor axes (at a distance of 16.8 Mpc), while the diffuse source in NGC 6500 has a diameter of ~ 90 pc (at a distance of 40 Mpc).

The UV images of NGC 5005 and NGC 7743 show very faint excesses over the background level at the positions of the optical nuclei. These features are not likely to be due solely to noise or cosmic rays, as they are located precisely at the positions of the optical nuclei and they appear to be diffuse sources, rather than residual cosmic-ray spikes. From our photometry, we estimate the significance of these detections to be 6σ for NGC 7743 and 4σ for NGC 5005, as measured in a 7×7 pixel detection aperture. A diameter of 7 pixels for these sources corresponds to physical dimensions of 33 pc and 38 pc, respectively, at distances of 21.3 Mpc and 24.4 Mpc for NGC 5005 and NGC 7743.

We determined upper limits to the F218W count rates of the undetected galaxies by examining the noise level of the images and by artificial star tests, assuming point-source profiles. The two major sources of noise in the UV images are readout noise and cosmic-ray residuals. The mean background noise level measured in the UV images (after cosmic-ray removal and averaging of sub-exposures) is 0.75 counts pixel⁻¹, with a dispersion of 0.10 counts pixel⁻¹ among the images. As the noise properties of all the UV images are similar, we assume for simplicity that all images of undetected galaxies have $\sigma = 0.75$ counts pixel⁻¹. Then, the 3σ upper limit to the flux of a UV point source in the undetected galaxies is 10 total counts within a detection aperture of $r = 2$ pixels. We also experimented with adding artificial stars with a range of magnitudes to the images, and found that stars with 10 total counts were not always found by eye, while stars with 20 or more total counts were consistently detectable. We therefore adopted 20 total counts as our conservative upper limit to the flux of any nuclear UV point source in the undetected galaxies. This count limit was then converted to flux limits in the same manner as described above, and the results are given in Table 2.

One further concern is the red leak of the F218W filter, particularly for such weak detections as NGC 5005 and NGC 7743. The F218W transmission curve extends to ~ 5000 Å, and for our purposes, we will consider the red leak contribution to be the count rate measured through the F218W filter due to photons with $\lambda > 3000$ Å. Applying the measured transmission curve

to a variety of stellar and galactic spectra in SYNPHOT, we determined the expected red leak contribution as a function of spectral type. The fractional contribution of red leak to the total F218W count rate ranges from 0.3% for an A0 star to 58% for an M6 star. For a template UV-optical spectrum of an S0 galaxy (provided by D. Calzetti), which should be a reasonable match in overall color to most of the galaxies in our sample, the red leak contribution to the F218W count rate is 2% and the ratio of the F547M count rate to the F218W red leak count rate is 1×10^5 . Most galaxies in our sample have F547M count rates of $\lesssim 3$ counts s^{-1} in the peak pixel; the implied red leak count rate of $\lesssim 3 \times 10^{-5}$ counts s^{-1} is far too small to be detectable in exposure times typical of our sample. For example, the brightest pixel in the nucleus of NGC 4203 has 4.2 counts s^{-1} in F547M and 0.04 counts s^{-1} in F218W; if our estimates based on the S0 template spectrum are roughly correct, then the red leak contribution to the F218W count rate should be $\sim 0.1\%$, or less than one count in the peak pixel. Based on these estimates, we are confident that the effects of red leak are insignificant in our data.

The total UV detection rate for our sample is 30%, while the FOC survey of Maoz et al. found a detection rate of 20% for LINERs and LINER/H II transition galaxies. The greater detection rate in the WFPC2 sample may be in part due to the longer integrations and post-refurbishment optics. A further advantage of the current survey is that the optical images allow us to find the exact locations of the nuclei in the UV images, hence we are able to identify very weak nuclear sources such as those in NGC 5005 and NGC 7743 which might otherwise have gone unnoticed. If we had not detected these two very faint sources, our detection rate would have been 20%. Combining the WFPC2 and FOC samples, there are 24 objects classified as LINERs, and six are detected in the UV, for an overall detection rate of 25%.

3.2. Host Galaxy Inclinations and Obscuration

The results of Maoz et al. (1995) and of this survey indicate that UV emission is not detected in the majority of LINERs. To what extent might dust obscuration be responsible for this fact? One straightforward way to test the obscuration hypothesis is to compare the host galaxy inclinations of the UV-detected and the UV-undetected objects. To improve the statistical significance of our results, we have combined our WFPC2 sample with the sample of Maoz et al., selecting only spiral and S0 hosts for which an inclination can be meaningfully measured. The results are shown in Figure 4, for all galaxies in the combined WFPC2 + FOC sample (excluding ellipticals), and also for the subset of these galaxies which are classified as pure LINERs.

It is immediately clear that the distributions of inclination are different for the UV-detected and undetected galaxies. In the entire sample, the mean inclination for UV-detected galaxies is 40° , while for UV-undetected galaxies the mean inclination is 63° . For the LINERs-only subsample, the corresponding figures are 35° and 62° , respectively. No galaxy with $i > 65^\circ$ is detected in the UV, while 4 out of 6 LINERs with $i < 45^\circ$ are detected. Applying the Kolmogorov-Smirnov (KS) test, we find a probability of $P_{KS} = 1.6\%$ that the distributions of inclinations for UV-detected and

undetected galaxies could be drawn from the same parent population, or 1.8% for the LINERs-only subsample. Detection of a UV source is thus significantly more likely in a low-inclination host than in a highly inclined host, and obscuration by dust is the most plausible explanation. Since 2/3 of LINERs with $i < 45^\circ$ are detected, it is reasonable to suppose that the true fraction of LINERs having UV sources at their nuclei is $\gtrsim 2/3$, but that extinction hides the majority of the UV sources from our view.

To further test the obscuration hypothesis, we have compared the Balmer decrements of the UV-detected and undetected LINERs, using the line ratio data of Ho et al. (1997a), which have been corrected for Galactic reddening using the Burstein & Heiles (1984) correction factors. In order to remove possible sources of bias from the comparison, we include only objects which are classified as LINERs by Ho et al. (1997a). The comparison is complicated by the fact that for a few objects, the measured Balmer decrements are unphysical; that is, $H\alpha/H\beta < 2.8$, sometimes by a large margin. Uncertainty in the starlight subtraction procedure is the most likely cause of these anomalous results, particularly for galaxies with extremely weak $H\beta$ emission. To minimize the influence of unphysical values on the sample properties, we have computed median, rather than mean, values of the Balmer decrements. In the combined WFPC2 + FOC sample, the UV-detected LINERs have a median $H\alpha/H\beta$ of 3.18 (for 6 objects), while the UV-undetected LINERs have a median $H\alpha/H\beta$ of 4.33 (18 objects). Among the UV-detected LINERs, the largest Balmer decrement is 3.51 (for NGC 404), while 70% of the UV-undetected LINERs have Balmer decrements greater than 3.5. The distributions of $H\alpha/H\beta$ for the UV-detected and undetected objects are shown in Figure 5, and the KS test indicates that the distributions are different at the 99% confidence level ($P_{KS} = 0.01$).

The median Balmer decrement of 4.33 for the UV-undetected LINERs implies an extinction of $A_V = 1.1$ mag, or 3.5 mag of extinction at 2200 Å. Such a large extinction would be more than sufficient to completely hide from view UV sources as bright as those in NGC 3642 and NGC 4203. We conclude that the UV-undetected LINERs are on average more highly reddened by dust within the host galaxies than the UV-detected LINERs, and that internal reddening is likely to be the primary reason for the low UV detection rate.

3.3. Equivalent Widths and Emission-Line Ratios

Inspection of the optical spectra presented by Ho et al. (1995) reveals a striking difference between the UV-detected and undetected LINERs: in nearly all of the UV-detected LINERs, [O III] is reasonably strong and stands out clearly above the continuum, while in nearly all of the UV-undetected objects, [O III] and $H\beta$ appear to have equivalent widths (EWs) so small that without starlight subtraction it would be impossible to measure their strengths at all. To quantify this result, we show in Figure 6 the distributions of EW for $H\beta$, [O III], and $H\alpha$ for the UV-detected and undetected LINERs. Median values of the EWs are listed in Table 3. The KS test confirms that the detected and undetected subsamples have different distributions of EW, at least for [O III]

and $H\beta$: $P_{KS} = 0.019, 0.039, \text{ and } 0.14$, respectively, for $H\beta$, $[O\ III]$, and $H\alpha$. This result indicates that LINERs with greater emission-line EWs are more likely to be detected in the UV.

We have also examined the distributions of other emission-line ratios in order to search for other differences between the UV-detected and undetected LINERs. Using data from Ho et al. (1997a), we have compiled the ratios $[O\ III]\ \lambda 5007/H\beta$, $[O\ I]\ \lambda 6300/H\alpha$, $[N\ II]\ \lambda 6583/H\alpha$, and $[S\ II]\ \lambda\lambda 6716, 6731/H\alpha$, corrected for both Galactic and internal reddening. To avoid biases due to a heterogeneous sample, only objects classified as LINERs have been included. Three objects (NGC 5195, NGC 5322, and NGC 7814) were omitted because some lines were not detected in their spectra. Six UV-detected and 15 UV-undetected LINERs remain in the sample. The distributions of line ratios for the UV-detected and undetected objects are shown in Figure 5, and the median values of each distribution are listed in Table 3. We note that the distribution of Hubble types does not differ significantly between the UV-detected and undetected LINERs, so that metallicity differences due to host galaxy type should not affect the comparison.

To quantify whether there are any meaningful differences between the emission-line ratios of the UV-detected and undetected subsamples, we have applied the KS test to each emission-line ratio distribution; the results for each line ratio are listed in Table 3. The KS test indicates that the $[O\ I]/H\alpha$ and $[S\ II]/H\alpha$ ratios do not significantly differ between the UV-detected and undetected LINERs. The median $[N\ II]/H\alpha$ ratio is larger for the UV-undetected than the UV-detected LINERs (1.84 vs. 1.29), but the difference between the two distributions is not highly significant ($P_{KS} = 0.16$). A significant difference is found for $[O\ III]/H\beta$: the UV-detected LINERs have median $[O\ III]/H\beta = 1.44$, while the undetected LINERs have median $[O\ III]/H\beta = 1.85$, and the KS test yields a 98.6% confidence level that the two distributions are different.

A greater contribution from stellar photoionization in the UV-detected LINERs could be responsible for the lower $[O\ III]/H\beta$ ratio in these objects. The emission-line data of Ho et al. (1997a) indicate that the mean $[O\ III]/H\beta$ ratio for H II nuclei is 0.81, while for LINERs in spiral hosts, the mean is 1.89. Furthermore, the median $EW(H\alpha)$ for LINERs in spiral hosts is 2.2 Å, while H II nuclei have a considerably larger median $EW(H\alpha)$ of 17.7 Å. A greater contribution of stellar photoionization in the UV-detected LINERs would decrease $[O\ III]/H\beta$, $[O\ I]/H\alpha$, $[N\ II]/H\alpha$, and $[S\ II]/H\alpha$, while at the same time increasing $EW(H\alpha)$ and $EW(H\beta)$, consistent with our results. However, because most of the UV-undetected LINERs have very low EWs of $H\beta$ and $[O\ III]$, we are cautious about interpreting the observed difference in the $[O\ III]/H\beta$ ratio between the UV-detected and undetected subsamples. Uncertainties in the starlight subtraction procedure, which are extremely difficult to quantify, could lead to biases in the measured ratio of two extremely weak emission lines, and it is possible that such biases could substantially affect the measured line ratios.

3.4. Broad H α Emission

One prediction of the duty cycle hypothesis of Eracleous et al. (1995) is that UV emission and broad H α emission should occur simultaneously. In this model, the broad-line emission, which originates within a few light-days of the nucleus, disappears rapidly if the ionizing continuum shuts off. A correlation between the presence of broad H α emission and UV emission would also be expected in an obscuring torus scenario, at least for those LINERs which are AGNs, since the UV and broad-line emission would both originate from regions which are small compared with the size of the obscuring torus. Using the broad H α measurements of Ho et al. (1997b), we have compared the UV and broad-line properties of the galaxies in our sample.

In the combined WFPC2 + FOC sample, including all galaxies (LINER, transition, and Seyfert nuclei), the UV-detected galaxies are indeed more likely to host broad H α emission than are the UV-undetected galaxies. Of the UV-detected galaxies (10 total), 4 have broad H α , while only 3 of the 28 UV-undetected galaxies, or 11%, have broad H α . Restricting the sample to LINERs only, broad H α emission occurs in 3 out of 6 UV-detected galaxies but only in 4 out of 18 UV-undetected galaxies.

This result offers support to models in which UV and broad-line emission are expected to occur together. However, the interpretation is complicated by the fact that some of the detected UV sources are extended or diffuse regions, in which there is no clear evidence for an AGN-like UV point source. If the spatially extended UV sources are clusters of hot stars, rather than AGNs, then one would not necessarily expect broad H α emission to be associated with the UV sources. Another possibility is that the spatially extended UV emission may be scattered radiation from an obscured AGN. This possibility can be tested with polarimetric observations, and in this case the UV emission could be accompanied by scattered broad H α emission as well.

The two galaxies in our sample with unresolved nuclear UV sources (NGC 3642 and NGC 4203) both have broad H α emission. Thus, there may be an even stronger likelihood for broad H α emission to be found in nuclei having *pointlike* UV emission, but our sample is not large enough to address this question properly. Also, because our sample was selected to exclude galaxies with strong broad H α emission, the rate of detection of UV emission may be lower in our sample than it would be in an unbiased sample of LINERs.

3.5. Optical Morphology

The most striking feature of the optical images is the nearly ubiquitous presence of optically thick dust lanes in most of the sample galaxies. Particularly intriguing is the fact that the dust lanes occur in very early-type spirals such as NGC 3607 (S0) and NGC 3166 (S0/a). The prevalence of dust in the nuclei of early-type spirals has been noted in WFPC1 imaging surveys (e.g., Phillips et al. 1996), but the WFPC2 images show the dust lanes in great detail. In the most extreme cases,

such as NGC 3166 and NGC 3607, the contrast between adjacent bright and dark regions in the F547M images is as much as a factor of 2 (i.e., $A_V=0.75$ mag). Assuming for simplicity that the geometry of the absorbing dust is a uniform screen, the corresponding extinction at 2200 Å is a factor of 8.8, or 2.4 mag. UV sources as bright as those in NGC 3642 or NGC 4203 would be below our detection threshold if they were located behind such a large obscuring column.

Detailed surface photometry of the optical images will be presented elsewhere, but one aspect of the optical images that is relevant for this study is the “peakiness” of the optical nuclei. In a study of WFPC1 images of Markarian Seyferts, Nelson et al. (1996) have shown that the nuclear profiles of the Seyfert 1 galaxies are significantly sharper and more pointlike than those of the Seyfert 2s. Their result adds support to unified models for Seyferts, since the unified schemes predict that the central source is viewed directly in Seyfert 1s but blocked by obscuring material in Seyfert 2s. We have examined the optical nuclear profiles of the galaxies in our sample, in order to determine whether such a clear difference exists between the type 1 and type 2 LINERs or between the UV-detected and undetected LINERs. The two objects in our sample having pointlike UV emission and broad H α emission, NGC 3642 and NGC 4203, appear to have particularly sharply peaked optical nuclei, compared to most other galaxies in the sample, suggesting that the correlation found for Markarian Seyferts may extend to the LINERs as well.

To quantify the “peakiness” of the nuclei, we have used a sharpness parameter adapted from Nelson et al. (1996), and defined as

$$S = \frac{\sum_i C_i^2}{(\sum_i C_i)^2}, \quad (1)$$

where C_i is the number of counts in pixel i , and the sum is taken over a square aperture surrounding the nucleus². This quantity measures the contrast in count rates within an aperture without making any assumptions about the spatial profile of the source. In the limiting cases of a source with uniform surface brightness or of a delta-function source, the sharpness parameter will be $1/N$ (where N is the total number of pixels within the aperture) or 1, respectively. Sharpness measurements were made in apertures of 3×3 and 7×7 pixels centered on the nuclei of the galaxies. In a few objects (NGC 2655, 3166, 3607, and 5005), it is unclear whether the nucleus itself is visible, and we have centered the aperture on the brightest pixel in the nuclear region. The sharpness measurements are listed in Table 2. For comparison, an artificial PSF has $S(3 \times 3) = 0.19$ and $S(7 \times 7) = 0.11$. In contrast to the Markarian Seyfert 1s, many of which have very sharply peaked nuclei (Nelson et al. 1996), most galaxies in our sample have sharpness values only slightly greater than those expected for uniform distributions. This result reflects the fact that the central sources are generally of low luminosity and lie within strong backgrounds of bulge starlight.

Despite the fact that the sharpness values are low for all galaxies in the sample, some systematic

²Nelson et al. (1996) measure the sharpness parameter over a circular aperture, while we have used a square aperture for simplicity.

trends are apparent. The median sharpness of the UV-detected galaxies is greater than that of the undetected objects (0.1182 vs. 0.1127 in a 3×3 pixel aperture), and the KS test shows that the difference between the two distributions is significant at the 93% confidence level. Similarly, the objects in our sample having broad H α emission have sharper nuclei than galaxies with no broad H α (0.1178 vs. 0.1128 in a 3×3 pixel aperture), with a 90% confidence level for a significant difference between the two distributions. For the Markarian Seyferts, Nelson et al. interpreted their results in terms of the effects of the obscuring torus; in the type 2 Seyferts, the line of sight to the nucleus is blocked by the parsec-scale torus, resulting in the diffuse nuclear morphology. Among the LINERs, however, the most diffuse nuclei in our sample are those in which the nuclei are clearly obscured by 100-pc scale dust lanes, such as NGC 3166 and NGC 3607. Obscuring tori may occur at smaller scales, but the optical nuclear sharpness of LINERs may be largely determined by the presence or absence of large-scale dust lanes covering the nuclei.

4. Discussion

One of the key questions we wish to address is whether any of the LINERs in our sample may have nonstellar, AGN-like UV continua. The discovery of compact UV sources in NGC 3642 and NGC 4203, in addition to the broad H α line observed in these galaxies, suggests that these objects may be true low-luminosity AGNs. If we speculate that the compact UV sources in these two galaxies may have nonstellar, power-law spectra, are their extrapolated ionizing luminosities sufficient to power the observed LINER emission? Following the analysis of Maoz et al. (1995), we calculate the ratio $N_{ion}/N_{H\alpha}$, where N_{ion} is the number of ionizing photons extrapolated from the 2200 Å flux, assuming an $f_\nu \propto \nu^{-1}$ continuum, and $N_{H\alpha}$ is the number of H α photons emitted. For Case B recombination, $N_{ion}/N_{H\alpha} = 2.2$ if all ionizing photons are absorbed in the narrow-line region (NLR) (Osterbrock 1989). Using the extinction-corrected H α fluxes measured by Ho et al. (1997a), we find $N_{ion}/N_{H\alpha} = 2.4$ and 3.2 for NGC 3642 and NGC 4203, respectively, indicating a surplus of ionizing photons with respect to the minimum number required to produce the observed H α emission. Such a comparison is complicated by the uncertainty in the extinction toward the central source as well as by calibration uncertainties in the optical spectrophotometry (e.g., slit losses; see Ho et al. 1997a for a discussion), but the fact that $N_{ion}/N_{H\alpha} > 2.2$ in both cases demonstrates that nonstellar photoionization is a plausible mechanism for the excitation of the NLRs of these galaxies. The most important caveat to this conclusion is that UV spectroscopy is needed to test whether the UV continua are indeed nonstellar. It is quite possible that these sources may be young star clusters; *HST* imaging has shown that many nearby galaxies contain near-nuclear star clusters with sizes of only a few pc and UV luminosities comparable to those of the nuclear sources in NGC 3642 and NGC 4203 (Meurer et al. 1995; Maoz et al. 1996).

The energy budgets of NGC 6500 and NGC 4569 have been discussed by Barth et al. (1997) and Maoz et al. (1998). Massive stars alone cannot provide the power required to ionize the NLR in NGC 6500, and an additional ionization mechanism must be present, presumably shocks or an

obscured AGN. In NGC 4569, the young stellar population appears to be just sufficient to power the emission lines, provided that very massive stars are still present in the cluster (Maoz et al. 1998). No UV spectral information is available for NGC 5005 or NGC 7743. However, if we speculate that the LINER NGC 5005 may have a UV spectral shape similar to that of NGC 4569 and the other LINERs studied by Maoz et al. (1998), then it suffers from a severe deficit of ionizing photons. Its nuclear UV source is too weak by more than an order of magnitude to power the NLR luminosity, and another energy source must be present in addition to the hot stars that presumably provide the observed UV continuum. If we assume that the UV continuum in the Seyfert 2 galaxy NGC 7743 is also produced by an extremely young starburst, then after correcting for the very substantial internal reddening ($H\alpha/H\beta= 5.85$), the UV continuum would be energetically sufficient to power the narrow-line emission. However, it is unlikely that hot stars alone could produce the higher-ionization Seyfert 2 narrow-line spectrum, and scattered AGN UV continuum radiation, which has been detected in other Seyfert 2 nuclei (e.g., Pogge & De Robertis 1993), could be the source of the spatially extended UV emission.

If the UV-undetected galaxies are simply obscured versions of the UV-detected galaxies, then some of them could also be powered by nonstellar photoionization. Observations at other wavebands will be necessary to determine the nature of these objects: for example, hard X-ray emission or compact radio sources can reveal the presence of a hidden AGN.

The possible role of shock excitation within LINER nuclei remains unclear. The simulations of Dopita & Sutherland (1995, 1996) have shown that fast shocks can closely reproduce the optical spectra of LINERs, but UV emission-line spectroscopy is a more definitive test of the shock hypothesis. At present, the only LINER known to have UV emission-line ratios consistent with the shock models is the nuclear disk of M87 (Dopita et al. 1996), and UV spectroscopy of more objects is clearly needed to determine whether other LINERs may be excited by shocks. Because shocks produce little UV continuum emission, obtaining UV spectra of *UV-undetected* LINERs to search for high-excitation emission lines is perhaps the best way to assess the importance of shock heating in LINERs. Such a test is possible with the Space Telescope Imaging Spectrograph (STIS). Morse, Raymond, & Wilson (1996) have also pointed out that the *HST* F220W filter passband contains several UV emission lines which are expected to be strong in fast shocks (as in the models of Dopita & Sutherland 1996), and which might contribute to a spatially extended component of the UV emission detected in *HST* images; again, UV spectroscopy of more LINERs is needed to test this possibility.

The observed inclination dependence of the UV detection rate echoes similar results that have been obtained for Seyfert nuclei. Keel (1980) found that Seyfert 1 nuclei are preferentially found in face-on hosts. This result was extended by Kirhakos & Steiner (1990), McLeod & Rieke (1995), and Maiolino & Rieke (1995), who demonstrated that Seyfert 2 nuclei avoid edge-on hosts as well, and by Simcoe et al. (1997), who have shown that the distribution of soft X-ray selected Seyferts is biased against edge-on hosts. The consensus of these studies is that the NLR is typically surrounded by optically thick obscuring material, which must be preferentially aligned with the galactic plane

in a geometrically thick torus-like structure denoted the “outer torus” by Maiolino & Rieke (not to be confused with the inner, parsec-scale torus surrounding the broad-line region). This outer, 100-pc scale torus of obscuring material prevents the optical or UV detection of Seyfert nuclei in edge-on or nearly edge-on hosts. The question of whether LINERs are preferentially found in face-on hosts is beyond the scope of this paper, but the fact that UV sources are not detected in edge-on LINERs suggests that the thick outer torus scenario proposed for Seyferts may apply to LINERs as well. If we take 65° as the maximum inclination at which UV sources may be detected, then the thickness-to-radius ratio of the outer torus is roughly unity. The obscuration need not be in any kind of organized structure such as a torus, however. The optical images suggest that the morphology of the obscuring clouds is in most cases far more irregular, patchy, or filamentary than a simple torus model. Two galaxies in our sample, NGC 3607 and NGC 7217, do have well-defined dust rings, although it is not clear whether the vertical structure of these rings is thick or flattened.

Infrared (IR) observations could be used to quantify the dust content of the nuclei, but sufficient IR data do not yet exist to study the entire sample. The spatial resolution of *IRAS* measurements is too coarse to isolate the nuclei on the relevant scales of 100 pc or less. It would be interesting to compare the optical dust-lane properties with ground-based small-aperture mid-IR measurements, but such detections have been reported for fewer than half of the galaxies in this sample (see Giuricin et al. 1994 for a compilation of 10 μm measurements of nearby galactic nuclei).

Since our results imply that the majority of LINERs contain nuclear UV sources, most of which are obscured by dust, there is no need to invoke a low AGN duty cycle, as in the hypothesis of Eracleous et al. (1995), to explain the low UV detection rate. However, even if the rate of stellar breakup flashes is not the explanation for the UV detection rate, the recent appearance of broad double-peaked $\text{H}\alpha$ emission in the LINERs NGC 1097 (Storchi-Bergmann, Baldwin, & Wilson 1993), Pictor A (Halpern & Eracleous 1994), and M81 (Bower et al. 1996) serves as an important reminder that such accretion events may contribute significantly to the energetics of LINERs.

5. Conclusions

Our discovery that the probability of detection of UV emission in a LINER is dependent on the host galaxy inclination and internal reddening provides a straightforward explanation for the low UV detection rate of LINERs. Nearly all of the UV-detected LINERs are in low-inclination, low-extinction hosts, while *no* LINERs in highly inclined ($i > 65^\circ$) or highly reddened ($\text{H}\alpha/\text{H}\beta > 3.6$) hosts are detected in the UV. The optical images show that many low-inclination galaxies (such as NGC 3607) have optically thick dust lanes covering the nuclei which could easily obscure a UV source; thus, the fraction of LINERs that contain nuclear UV sources is likely to be greater than the observed fraction, even among low-inclination hosts. Since two-thirds of LINERs with $i < 45^\circ$ are detected in the UV, it seems reasonable to take this ratio as a lower limit to the detection rate we would obtain in the absence of any obscuration. The dependence of UV detection rate on emission-line equivalent width is also easily understood if the obscuring material blocking our

view of the UV-undetected nuclei also obscures part of the NLRs in these galaxies, and if the emission-line luminosity of LINERs is correlated with their UV luminosity.

If the pointlike UV sources in NGC 3642 and NGC 4203 are AGNs, their extrapolated continua are energetically sufficient to account for the emission-line luminosities of the NLRs of these galaxies. This result supports the hypothesis that at least some LINERs may be primarily photoionized objects which are low-luminosity examples of the AGN phenomenon.

Spectroscopy is needed to determine the origin of the UV emission, which may arise from low-luminosity AGNs or compact young star clusters. The model of Eracleous et al. (1995), in which *all* the differences between UV-detected and undetected LINERs can be ascribed to AGN duty cycles, does not account for the observed dependence of detection rate on inclination, or for the fact that some UV sources in LINERs are likely to be young star clusters. Although duty cycles may occur in those LINERs which are AGNs, dust obscuration is likely to be the dominant factor determining whether a UV source is visible.

We are grateful to Dan Maoz for supplying data on the FOC sample of LINERs, and to Daniela Calzetti for providing template galaxy spectra. Mike Liu provided valuable assistance and advice on image processing. Support for this work was provided by NASA grant NAG 5-3556, and by NASA grant GO-5419.02-93A from the Space Telescope Science Institute, which is operated by AURA, Inc., under NASA contract NAS 5-26555. L. C. H. acknowledges fellowship support from the Harvard-Smithsonian Center for Astrophysics. This research has made use of the NASA/IPAC Extragalactic Database (NED), which is operated by the Jet Propulsion Laboratory, California Institute of Technology, under contract with NASA.

Appendix A. Notes on Individual Galaxies

NGC 2655– Dust lanes cross the nuclear region of this Seyfert 2 galaxy. The true nucleus may be heavily obscured.

NGC 3607– The F547M image clearly shows the circumnuclear dust ring described by Singh et al. (1994), as well as a thick filament of dust crossing over the nucleus itself. The inner radius of the dust ring is $3''$, or ~ 300 pc. Singh et al. conjecture that the nuclear dust was accreted during a recent interaction with the nearby companion NGC 3608.

NGC 3642– Compact UV emission and broad $H\alpha$ emission make this galaxy an excellent example of an AGN-like LINER. A compact nuclear X-ray source with a power-law spectrum was detected by Koratkar et al. (1995).

NGC 3718– This LINER has the highest nuclear sharpness of any galaxy in our sample, and is a source of broad $H\alpha$ emission, but no UV emission was detected.

NGC 4111– This S0 galaxy is nearly edge-on, with $i = 87^\circ$. Surrounding the bright, compact

nucleus is a dust lane oriented perpendicular to the galaxy’s plane; its morphology is suggestive of a polar ring having a radius of $3''$.

NGC 4192– This transition-type spiral is highly inclined ($i = 83^\circ$) and is heavily reddened internally ($H\alpha/H\beta = 14.3$ after removal of Galactic reddening), yet its optical nucleus is one of the sharpest in the sample.

NGC 4203– Like NGC 3642, this galaxy hosts a compact nuclear UV source and broad $H\alpha$ emission.

NGC 4569– Maoz et al. (1995) found the UV source in NGC 4569 to be pointlike, whereas in our image it is clearly extended even at the smallest radii, as illustrated in Figure 4. The most likely explanation for this discrepancy is that the FOC image of NGC 4569 was taken prior to the first *HST* refurbishment mission, and hence suffered from the aberrated *HST* PSF; it was also very heavily saturated, making profile measurements at small radii extremely difficult. Spacecraft jitter cannot be the cause of the spatial extent of the WFPC2 image, as the spatial profile is identical in the two UV exposures. The maximum possible contribution from a single point source in the WFPC2 image is 23% of the total flux, but the fluxes measured in the WFPC2 and FOC images differ by only 10%. The F547M image of NGC 4569 is saturated, and we are unable to measure the optical nuclear sharpness parameter for this object. The UV source has $S(7 \times 7) = 0.0489$, compared with $S(7 \times 7) = 0.1531$ for the synthetic F218W PSF, another indication that the UV profile of NGC 4569 is significantly more extended than a point source. The *IUE* and optical study by Keel (1996) demonstrated that the nucleus of this galaxy is a young star cluster 6 magnitudes more luminous than the core of 30 Doradus, and that the optical light from the cluster is dominated by A-type supergiants. *HST* data presented by Maoz et al. (1998) show that the UV spectrum is nearly an exact match to that of the young starburst cluster NGC 1741-B, which has a likely age of 4–5 Myr (Conti, Leitherer, & Vacca 1996).

NGC 5005– The optical morphology of the nucleus is suggestive of a clumpy, dusty starburst region. The faint patch of UV emission appears at the same location as the peak of the optical emission.

NGC 5195– This galaxy has been classified both as an amorphous irregular (I0) and as type SB. The LINER classification is uncertain, as the [O I] and [O III] lines are extremely weak.

NGC 6500– The nucleus of this LINER shows kinematic evidence for a nuclear outflow or wind; see González Delgado & Pérez (1996) for a discussion of the optical emission lines and kinematics. *HST* Faint Object Spectrograph data show that the UV continuum shape is consistent with that of a young stellar population with age $\lesssim 100$ Myr, and spectral features due to a young starburst may be weakly present (Barth et al. 1997; Maoz et al. 1998). The UV emission-line spectrum is of low excitation; C III] $\lambda 1909$, C II] $\lambda 2326$, and Mg II $\lambda 2800$ are the strongest collisionally excited lines in the spectrum, and C IV $\lambda 1549$ is not detected. At most $\sim 7\%$ of the UV emission from the nuclear region could be due to a single unresolved point source.

NGC 6951– This low-luminosity Seyfert 2 galaxy hosts a spectacular circumnuclear star-forming ring with projected dimensions of $1.0 \times 0.7 \text{ kpc}^2$. The structure of the ring and its compact star clusters are discussed by Barth et al. (1995).

NGC 7217– A dust ring of inner radius $6''.5$, or $\sim 500 \text{ pc}$, surrounds a nuclear region which appears to be nearly devoid of dust.

REFERENCES

- Barth, A. J., Ho, L. C., Filippenko, A. V., & Sargent, W. L. W. 1995, *AJ*, 110, 1009
- Barth, A. J., Reichert, G. A., Ho, L. C., Shields, J. C., Filippenko, A. V., & Puchnarewicz, E. M. 1997, *AJ*, in press
- Bower, G. A., Wilson, A. S., Heckman, T. M., & Richstone, D. O. 1996, *AJ*, 111, 1901
- Burstein, D., & Heiles, C. 1984, *ApJS*, 54, 33
- Cardelli, J. A., Clayton, G. C., & Mathis, J. S. 1989, *ApJ*, 345, 245
- Conti, P. S., Leitherer, C., & Vacca, W. D. 1996, *ApJ*, 461, L87
- de Vaucouleurs, G., de Vaucouleurs, A., Corwin, H. G. Jr., Buta, R. J., Paturel, G., & Fouqué, P. 1991, *Third Reference Catalogue of Bright Galaxies* (New York: Springer) (RC3)
- Dopita, M. A., & Sutherland, R. S. 1995, *ApJ*, 455, 468
- Dopita, M. A., & Sutherland, R. S. 1996, *ApJS*, 102, 161
- Dopita, M. A., et al. 1996, in *The Physics of LINERs in View of Recent Observations*, ed. M. Eracleous et al. (San Francisco: ASP), 44
- Eracleous, M., Livio, M., & Binette, L. 1995, *ApJ*, 445, L1
- Ferland, G. J., & Netzer, H. 1983, *ApJ*, 264, 105
- Filippenko, A. V., & Sargent, W. L. W. 1985, *ApJS*, 57, 503
- Filippenko, A. V., & Terlevich, R. 1992, *ApJ*, 397, L79
- Fosbury, R. A. E., Mebold, U., Goss, W. M., & Dopita, M. A. 1978, *MNRAS*, 183, 549
- Giuricin, G., Tamburini, L., Mardirossian, F., Mezzetti, M., & Monaco, P. 1994, *ApJ*, 427, 202
- González Delgado, R. M., & Pérez, E. 1996, *MNRAS*, 281, 1105
- Halpern, J. P., & Eracleous, M. 1994, *ApJ*, 433, L17

- Halpern, J. P., & Steiner, J. E. 1983, *ApJ*, 269, L37
- Heckman, T. M. 1980, *A&A*, 87, 152
- Ho, L. C., Filippenko, A. V., & Sargent, W. L. W. 1993, *ApJ*, 417, 63
- Ho, L. C., Filippenko, A. V., & Sargent, W. L. W. 1995, *ApJS*, 98, 477
- Ho, L. C., Filippenko, A. V., & Sargent, W. L. W. 1997a, *ApJS*, 112, 315
- Ho, L. C., Filippenko, A. V., Sargent, W. L. W., & Peng, C. Y. 1997b, *ApJS*, 112, 391
- Keel, W. C. 1980, *AJ*, 85, 198
- Keel, W. C. 1996, *PASP*, 108, 917
- Kirhakos, S. D., & Steiner, J. E. 1980, *AJ*, 99, 1435
- Koratkar, A., Deustua, S. E., Heckman, T. M., Filippenko, A. V., Ho, L. C., & Rao, M. 1995, *ApJ*, 440, 132
- Koski, A. T., & Osterbrock, D. E. 1976, *ApJ*, 203, L49
- Krist, J. 1994, *The Tiny Tim User's Manual* (Baltimore: STScI)
- Maiolino, R., & Rieke, G. H. 1995, *ApJ*, 454, 95
- Maoz, D., Filippenko, A. V., Ho, L. C., Rix, H.-W., Bahcall, J. N., Schneider, D. P., & Macchetto, F. D. 1995, *ApJ*, 440, 91
- Maoz, D., Filippenko, A. V., Ho, L. C., Macchetto, F. D., Rix, H.-W., & Schneider, D. P. *ApJS*, 107, 215
- Maoz, D., Koratkar, A., Shields, J. C., Ho, L. C., & Filippenko, A. V. 1998, *AJ*, submitted
- McLeod, K. K., & Rieke, G. H. 1995, *ApJ*, 441, 96
- Meurer, G. R., Heckman, T. M., Leitherer, C., Kinney, A., Robert, C., & Garnett, D. R. 1995, *AJ*, 110, 2665
- Morse, J. A., Raymond, J. C., & Wilson, A. S. 1996, *PASP*, 108, 426
- Nelson, C. H., MacKenty, J. W., Simkin, S., & Griffiths, R. E. 1996, *ApJ*, 466, 713
- Osterbrock, D. E. 1989, *Astrophysics of Gaseous Nebulae and Active Galactic Nuclei* (Mill Valley: University Science Books)
- Phillips, A. C., Illingworth, G. D., MacKenty, J. W., & Franx, M. 1996, *AJ*, 111, 1566
- Pogge, R. W., & De Robertis, M. M. 1993, *ApJ*, 404, 563

- Shields, J. C. 1992, ApJ, 399, L27
- Simcoe, R., McLeod, K. K., Schachter, J., & Elvis, M. 1997, ApJ, in press
- Singh, K. P., Prabhu, T. P., Kembhavi, A. K., & Bhat, P. N. 1994, ApJ, 424, 638
- Stetson, P. B. 1987, PASP, 99, 191
- Storchi-Bergmann, T., Baldwin, J. A., & Wilson, A. S. 1993, ApJ, 410, L11
- Terlevich, R., & Melnick, J. 1985, MNRAS, 213, 841
- Tully, R. B. 1988, Nearby Galaxies Catalog (Cambridge: Cambridge Univ. Press)
- Tully, R. B., & Shaya, E. J. 1984, ApJ, 281, 31

Note: Because of the large size of Figures 1 and 2, they are not included with the astro-ph distribution of this paper. They can be found at <http://astro.berkeley.edu/~barth/papers/uv>.

Figure 1– WFPC2/PC F218W images of the six UV-detected nuclei. Image size is $4.6'' \times 4.6''$. Logarithmic stretch was used for NGC 4569, and linear stretch for the other objects.

Figure 2– WFPC2/PC F547M images of the galaxies, rotated so that north is up and east is to the left. Images are $27'' \times 27''$ and are displayed with logarithmic stretch.

Table 1. The Galaxy Sample

Galaxy	Type	cz	i	$A_V(\text{Galactic})$	$H\alpha/H\beta$	Nuclear Type	Exp. Time (s)	
		(km s^{-1})	($^\circ$)	(mag)			F218W	F547M
NGC 1961	SABc	3934	54	0.29	5.44	L2	1800	300
NGC 2655	SAB0/a	1404	29	0.02	4.94	S2	1600	300
NGC 3166	SAB0/a	1345	58	0.01	6.50	L2	1800	300
NGC 3169	Sa pec	1233	59	0.03	5.03	L2	1600	300
NGC 3607	S0	935	30	0.00	5.56	L2	1600	260
NGC 3642	Sbc	1588	38	0.00	3.21	L1.9	1800	300
NGC 3718	SBa pec	994	66	0.00	4.33	L1.9	1800	300
NGC 3992	SBbc	1048	59	0.01	2.09	T2:	1400	230
NGC 4036	S0	1397	72	0.02	2.86	L1.9	1800	300
NGC 4111	S0	807	87	0.00	4.78	L2	1800	300
NGC 4192	SABab	-142	83	0.11	13.02	T2	1400	230
NGC 4203	SAB0	1086	26	0.00	1.03	L1.9	1800	300
NGC 4569	SABab	-235	64	0.07	4.90	T2	1400	230
NGC 4651	Sc	805	59	0.02	2.95	L2	1800	300
NGC 5005	SABbc	946	64	0.00	2.59	L1.9	1400	230
NGC 5195	SB0 pec	465	46	0.00	1.90	L2:	1400	230
NGC 6500	Sab	3003	46	0.28	3.31	L2	2200	350
NGC 6951	SABbc	1426	28	0.66	12.41	S2	2000	300
NGC 7217	Sab	946	32	0.31	6.83	L2	1800	300
NGC 7743	SB0	1710	38	0.13	5.85	S2	2000	300

Note. — Morphological types and heliocentric redshifts taken from NED. Inclinations (i) taken from Tully (1988), except for NGC 1961 and NGC 6500. For these galaxies, the inclination was calculated from the isophotal diameters given in the RC3 using the method described by Tully (1988). Galactic extinction (A_V) from Burstein & Heiles (1984). Balmer decrements ($H\alpha/H\beta$), corrected for Galactic reddening, taken from Ho et al. (1997a). Nuclear spectroscopic type from Ho et al. (1997a). L = LINER; T = LINER/H II “transition” type; and S = Seyfert. Colon indicates uncertain classification. The numerical classification indicates whether or not broad $H\alpha$ is detected (1.9 = weak detection; 2 = no detection).

Table 2. Measured Parameters

Galaxy	$f_{\lambda}(2200)$ (1)	$I_{\lambda}(2200)$ (2)	$100 \times S(3)$ (3)	$100 \times S(7)$ (4)
NGC 1961	< 2	< 4	11.29	2.20
NGC 2655	< 3	< 3	11.19	2.18
NGC 3166	< 2	< 2	11.12	2.05
NGC 3169	< 3	< 3	11.27	2.28
NGC 3607	< 3	< 3	11.15	2.07
NGC 3642	19	19	11.86	2.45
NGC 3718	< 2	< 2	12.95	2.84
NGC 3992	< 3	< 3	11.47	2.24
NGC 4036	< 2	< 2	11.28	2.18
NGC 4111	< 2	< 2	11.19	2.17
NGC 4192	< 3	< 4	12.18	2.54
NGC 4203	21	21	12.24	2.51
NGC 4569	1100	1300	... ^a	... ^a
NGC 4651	< 2	< 2	11.64	2.29
NGC 5005	6	6	11.78	2.22
NGC 5195	< 3	< 3	11.18	2.22
NGC 6500	27	57	11.18	2.08
NGC 6951	< 2	< 11	11.48	2.31
NGC 7217	< 3	< 5	11.27	2.11
NGC 7743	9	12	11.62	2.38

Note. — Columns (1) Measured flux at 2200 Å, corrected for WFPC2 internal throughput degradation, in units of 10^{-17} erg s⁻¹ cm⁻² Å⁻¹. (2) Flux corrected for Galactic extinction, in units of 10^{-17} erg s⁻¹ cm⁻² Å⁻¹. (3) 100× sharpness parameter measured in a 3 × 3 pixel aperture. (4) 100× sharpness parameter measured in a 7 × 7 pixel aperture.

^aF547M image saturated.

Table 3. Emission-Line Properties of UV-Detected and UV-Undetected LINERs

Quantity	Median Value for UV-Detected LINERs	Median Value for UV-Undetected LINERs	P_{KS}
$H\alpha/H\beta$	3.18	4.33	0.011
[O III] $\lambda 5007/H\beta$	1.44	1.85	0.014
[O I] $\lambda 6300/H\alpha$	0.24	0.25	0.86
[N II] $\lambda 6583/H\alpha$	1.29	1.84	0.16
[S II] $\lambda\lambda 6716, 6731/H\alpha$	1.22	1.37	0.76
EW($H\beta$) (\AA).....	2.41	0.62	0.019
EW([O III]) (\AA).....	3.36	1.23	0.039
EW($H\alpha$) (\AA).....	5.66	2.25	0.14

Note. — Emission-line data adapted from Ho et al. (1997a).

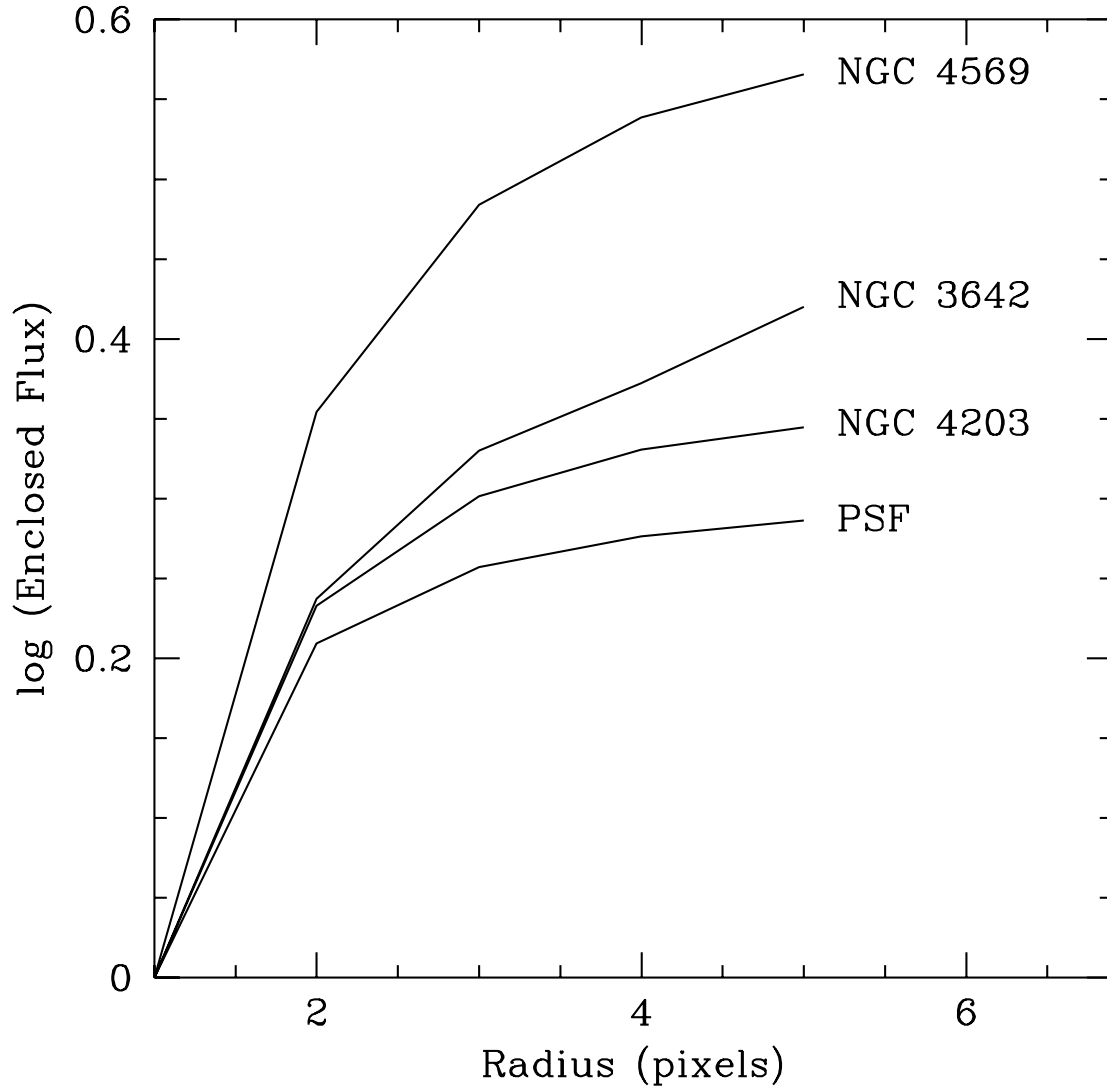


Fig. 3.— Photometric growth curves of the three compact UV sources and the artificial PSF, normalized to zero at $r = 1$ pixel radius. Note that NGC 3642 and NGC 4203 have nearly identical profiles within $r = 2$, while NGC 4569 is more extended than the PSF at all radii.

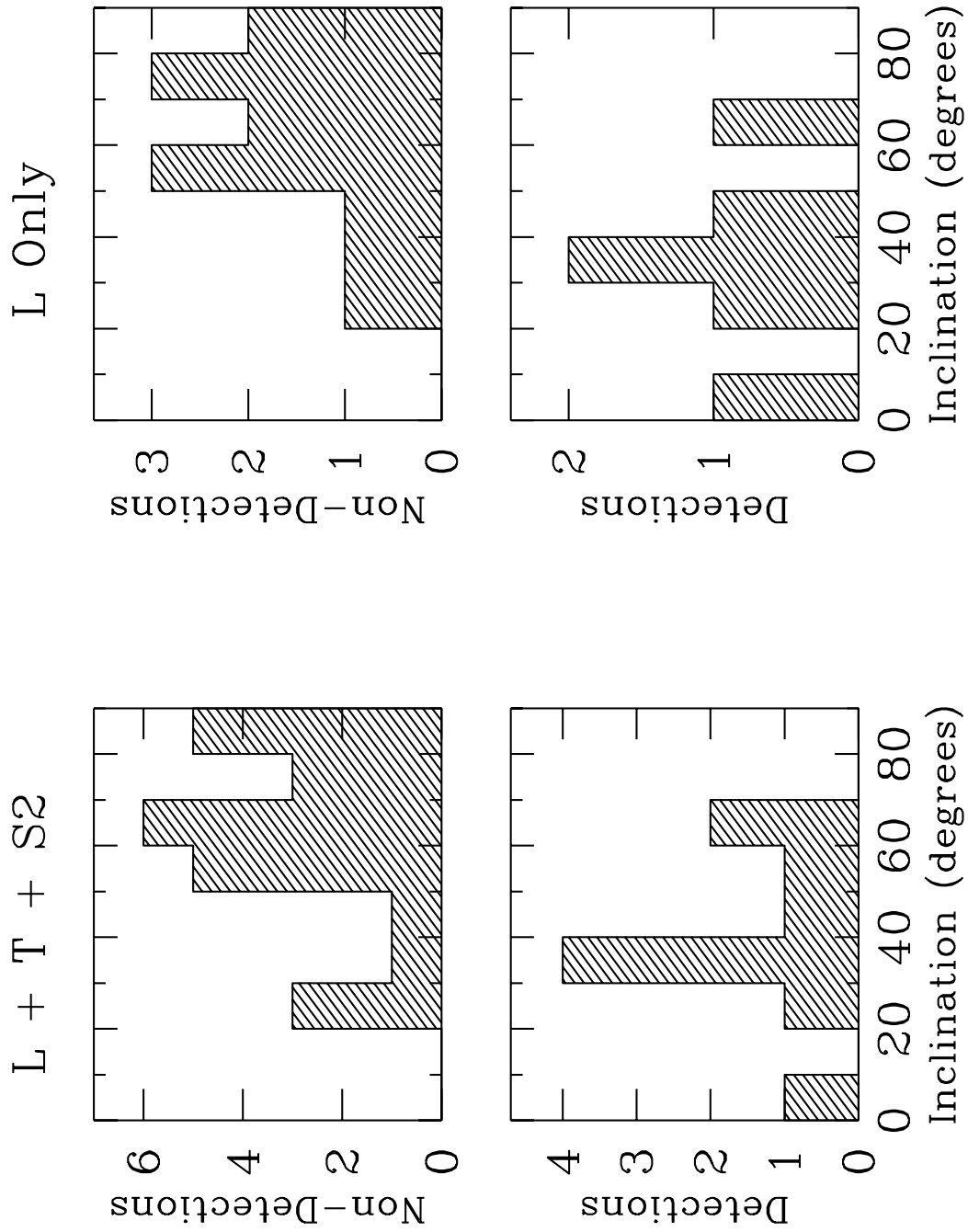


Fig. 4.— Histograms of host galaxy inclination, for spiral and SO hosts only. *Left panel*– LINERs, Seyferts, and “transition” type galaxies combined. *Right panel*– pure LINERs only.

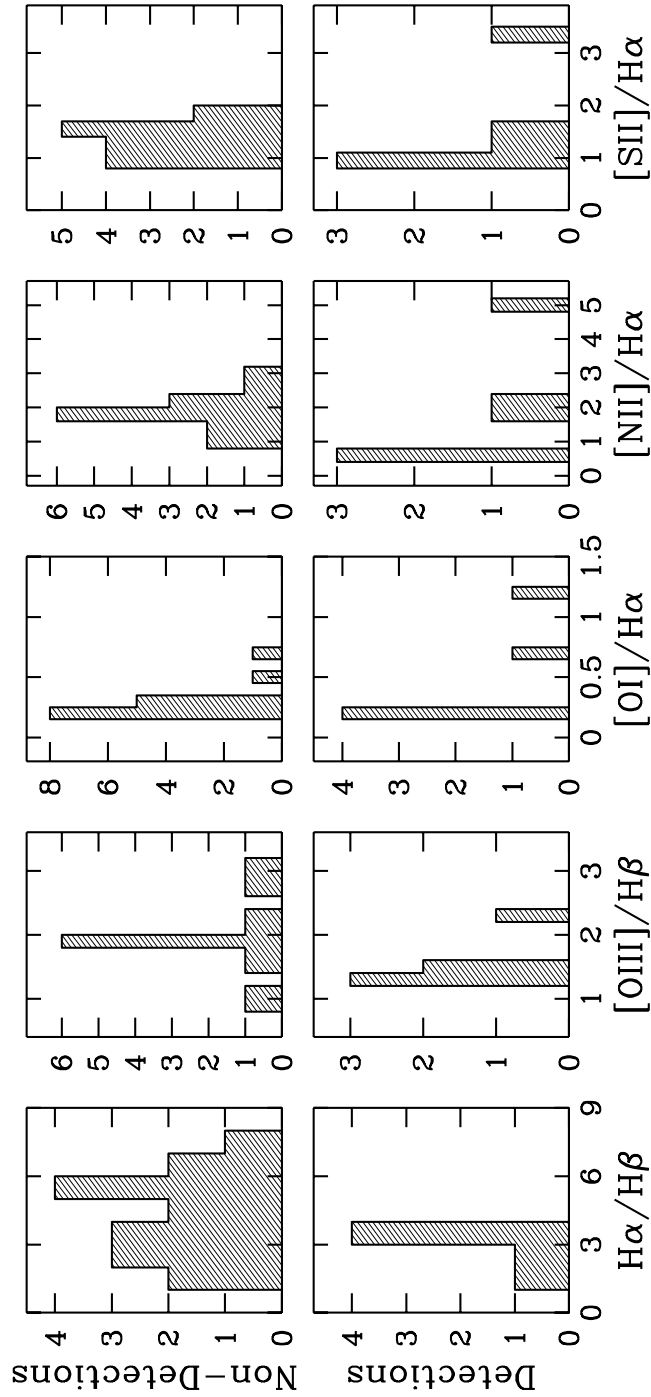


Fig. 5.— Emission-line ratios of UV-detected and undetected LINERs in the combined WFPC2 + FOC sample. Data adapted from Ho et al. (1997a). $H\alpha/H\beta$ has been corrected for Galactic extinction, and all other ratios have been corrected for both Galactic and internal extinction.

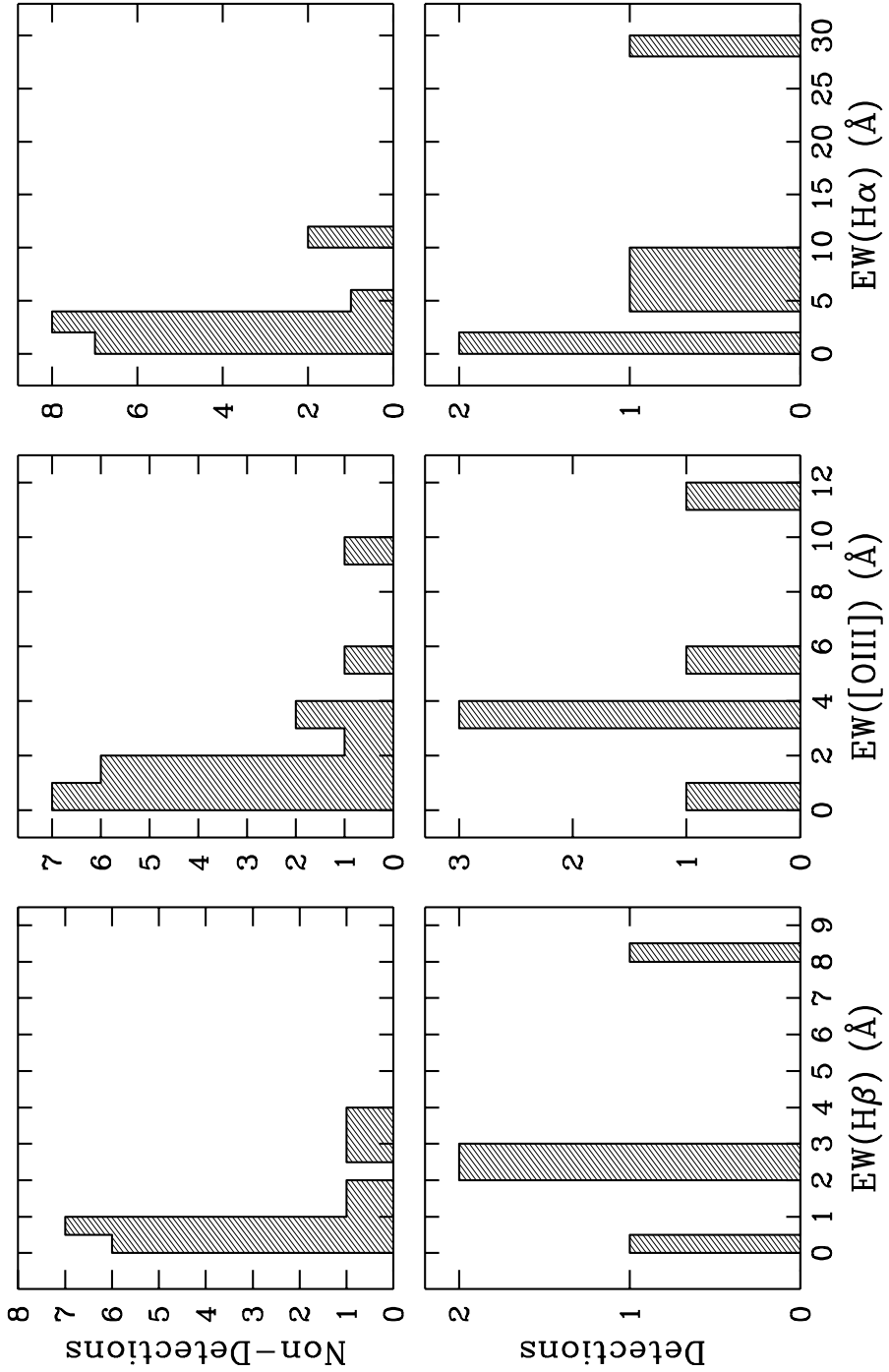


Fig. 6.— Equivalent widths of H β , [O III] λ 5007, and H α , for UV-detected and undetected LINERs in the combined WFPC2 + FOC sample. Data adapted from Ho et al. (1997a).